Establishing the ice strength coefficient from mean crushing loads and a theoretical velocity effect

Hornnes, Vegard; Hendrikse, H.; Høyland, Knut V.

27th IAHR International Symposium on Ice

Gdańsk, Poland, 9 – 13 June 2024

Establishing the ice strength coefficient from mean crushing loads and a theoretical velocity effect

Vegard Hornnes[1*], Hayo Hendrikse[2], Knut V. Høyland[1]
[1]*Norwegian University of Science and Technology, Department of Civil and Environmental Engineering,
Høgskoleringen 7A, 7491 Trondheim, Norway*
[2]*Delft University of Technology, Faculty of Civil Engineering and Geosciences,
Stevinweg 1, 2628CN Delft, The Netherlands*
**vegard.hornnes@ntnu.no
h.hendrikse@tudelft.nl
knut.hoyland@ntnu.no*

Abstract: The design of flexible vertical offshore structures exposed to crushing ice, such as offshore wind turbines, can become governed by ice loads and the structural response associated with low relative speeds between ice and structure. Low ice speeds can cause significant loads due to pressure synchronization and/or increase in contact, potentially larger than those observed at high ice speeds, which is often referred to as the velocity effect. In this study, the dataset from the full-scale measurement campaign at the Norströmsgrund lighthouse is reanalyzed. Several instances of ice load amplification are identified and presented, to confirm that synchronization and the velocity effect developed. The increase in ice load is quantified and discussed in the context of a theoretical framework, and model- and full-scale observations of the velocity effect on other structures. Then several events of high-speed crushing are investigated and the potential global pressures at low speeds for those events are estimated based on the theoretical framework. These estimates are compared to typical high-speed global crushing pressures used to define the ice strength coefficient C_R for the Baltic Sea. It is found that the velocity effect may produce global pressures equivalent to a C_R factor above 0.9 MPa. The results provide a theoretical substantiation for inclusion of the velocity effect and a possible physical interpretation of the recommended value of 1.8 MPa in the ISO 19906 design standard.

Keywords: Global ice loads; Ice-structure interaction; Velocity effect; Norströmsgrund lighthouse.

1. Introduction

The design of flexible vertical offshore structures exposed to crushing ice, such as offshore wind turbines, can become governed by ice loads and the structural response associated with low relative speeds between ice and structure. For deterministic design the ISO19906 (2019) crushing equation is often adopted which defines the characteristic design load as:

$$F_G = hwp_G, \tag{1}$$

where F_G is the peak global crushing load in continuous brittle crushing, h is the ice thickness, w is the structure width, or diameter in the case of a cylindrical structure, and p_G is the global pressure given by:

$$p_G = C_R \left[\left(\frac{h}{1}\right)^n \left(\frac{w}{h}\right)^m + f_{AR} \right], \tag{2}$$

with m an empirical coefficient equal to -0.16, n an empirical coefficient equal to $-0.5 + h/5$ for $h < 1.0\ m$, and -0.3 for $h \geq 1.0\ m$, C_R an ice strength coefficient, and f_{AR} an empirical term given by:

$$f_{AR} = e^{\frac{-w}{3h}} \sqrt{1 + 5\frac{h}{w}} \tag{3}$$

The crushing equation is valid for all velocities, and the ice strength coefficient C_R should incorporate the effects of natural variability of ice strength, exposure of the structure to sea ice, ice velocity (sometimes referred to as strain-rate) etc. For the Baltic Sea a nominal value of 1.8 MPa is defined for design purposes which is representative of a 1-year maximum accounting for all possible effects on the load and to be combined with relevant return period ice thickness values in the crushing equation (Kärnä and Masterson, 2011; ISO19906, 2019).

In a recent discussion paper, Hendrikse and Owen (2023) explored how the 'velocity effect', 'compliance effect' and 'dynamic amplification' are accounted for in the value of 1.8 MPa. Their analysis concluded that:

"When determining the design peak loads during intermittent crushing on the basis of the crushing equation in ISO 19906, it is important that the C_R coefficient used accounts for the velocity effect. The velocity effect herein refers to the observation that level or pack ice loads are generally largest for low far-field ice drift speeds or low relative velocity between ice and structure. For the Baltic Sea region, the nominal value of 1.8 MPa contains a factor to account for this effect."

What was not assessed in that work, is the consistency of the derivation of the C_R coefficient for the Baltic Sea and historical observations on the velocity effect. This question is relevant in the context of defining C_R values for the design of offshore wind turbines in the Baltic Sea. Currently, the commonly used approaches consist of using a subset of high-speed global crushing pressures measured on the Norströmsgrund lighthouse (Figure 1), fitting a statistical distribution to those, and estimating what certain return-period C_R values ought to be for a specific location with less or more ice exposure than the lighthouse (see for example Gravesen and Kärnä, 2009). The fact that these data concern only high-speed loading events (though this is not explicitly mentioned in the report by Kärnä and Qu (2006), or in any derivative papers) is then further either 1) not explicitly accounted for, or 2) accounted for by introducing

additional 'velocity safety factors' or 'compliance effect factors' which are either multipliers for C_R or included in advanced simulation models.
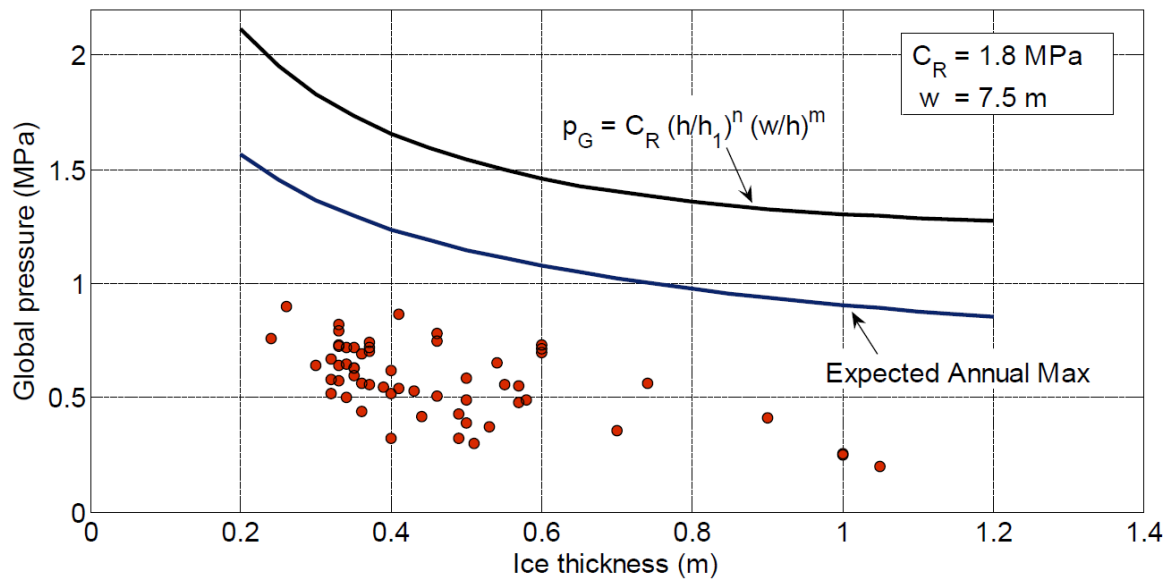

Figure 1. Global pressure data from the Norströmsgrund lighthouse as defined by Kärnä and Qu (2006). Note that the original report does not detail the exact events this data is associated with and hence the plot could not be reproduced. Adapted from Kärnä and Masterson (2011).

The approach sometimes leads to C_R values for design above 1.8 MPa and sometimes below 1.8 MPa. There are several challenges associated with this way of approaching the definition of C_R for design. The first is that it is not transparent what the design load level is due to the use of numerical models or structure dependent multiplication factors (compliance effect), as such the level of safety may vary from design to design. Second, there is no theoretical substantiation for the assumption that the exposure dependence of stochastic high speed crushing loads is like that of low-speed loads. Observations of intermittent crushing for example, suggest little dependence of peak loads on exposure. Third, the data points in Figure 1 are taken as given, without proper accounting of the uncertainty associated with those. There was no full panel coverage for the lighthouse, the panels only measured about 90% of the real load, and importantly the ice thickness measurements were not at the contact face and experienced high relative variability. Plots like the one in Figure 1 should have error bars indicating the sometimes up to 50% uncertainty in the position of some of the points, which directly affects any statistical analysis based on those.

Despite this, there is a reason for working with the high-speed crushing data. There are very few recordings of low speed synchronized loading on the lighthouse, thus little data to work with. Also, measurements on the lighthouse showed that the low speed synchronized loads were often not much higher than the high-speed loads. The latter can be explained by the relative rigidity of the structure, as is done in Section 3. To arrive at a value for design the more available recordings of high-speed stationary crushing were used, and later a factor was added to account for what was not measured, arriving at 1.8 MPa for the Bay of Bothnia in ISO 19906.

What does not seem to have been done before, is to interpret the data from the lighthouse in a theoretical framework that can explain both high-speed and low-speed loading effects, the velocity effect, and the development of ice-induced vibrations on flexible structures. In this paper we take this step based on recent model-scale developments (Owen et al., 2023) and the theoretical framework behind the ice model by Hendrikse and Nord (2019). In the framework,

the velocity effect reflects intrinsic ice deformation and failure behavior which can be observed on any structure (rigid or flexible) provided the relative velocity between ice and structure is low for a sufficiently long time. As such, all structures could experience a synchronization of pressures and/or contact area increase across the circumference during events with low-speed loading (such as stopping events), but the degree of synchronization depends on how long the low speed is maintained. If this is the case, very flexible structures can move with the ice thereby reducing the relative velocity between the two and allowing the ice to 'strengthen'. Rigid structures on the other hand require specific velocities to observe an increase in loading, which could for example occur when ice floes come to a very gradual stop.

Here we attempt to give an indication to what degree different values of C_R reflect different levels of synchronization. The levels are defined based on observations of synchronized behavior from a variety of structures (full-scale and model-scale) and related to the high-speed mean brittle crushing load in the same conditions. We analyze the global pressure data from the lighthouse to obtain high-speed mean brittle crushing pressure levels for its location.

This paper is structured as follows. First the full-scale data used in this paper is introduced and selection criteria for events are presented for reproducibility. Section 3 briefly introduces the theoretical framework and defines the ratio of the maximum low speed load to the mean load during high-speed crushing as a critical parameter based on model-scale and full-scale observations. In Section 4 this ratio is used in combination with high-speed crushing mean loads measured on the lighthouse to establish the range of low-speed loads that could have developed in the same conditions, provided a low interaction speed. These results are compared to the ice strength coefficient of 1.8 MPa as suggested in ISO 19906 and discussed in the last section.

2. Norströmsgrund lighthouse data

During the winters between 1999 – 2003, full-scale load- and environmental data were recorded as a part of the LOLEIF and STRICE campaigns at the lighthouse Norströmsgrund, located in the Bay of Bothnia (Schwarz and Jochmann, 2001; Bjerkås, 2006). Simultaneous load and environmental data from the campaigns were collated and cleaned of errors. Like in Hornnes et al. (2020), the recorded environmental data were interpolated using a previous neighbor interpolation routine. Further, to find brittle crushing events, the following selection criteria were applied to the time series:
- There is interpolated ice thickness data, which is above 0.1 m,
- There is interpolated ice velocity data above 0 m/s, or the velocity at the time could be substantiated from reports or observations at the lighthouse,
- The angle of approach is between 45 and 90 degrees (between north-east and east), to be confident that most of the global load is captured,
- Local panel loads are available.

Applying these selection criteria resulted in a reduced dataset of 75 time series. Further, to find the global load, the load on each panel was projected onto the reported ice drift direction and summed. That is, the load components orthogonal to the ice drift direction were not included in the global load. The loads were increased by 10% based on the load panel calibration report (Fransson, 2001). Then, we did a visual inspection to find stationary brittle crushing or ice stopping after crushing. For crushing events, that means there is at least one minute of continuous crushing without large fluctuations in mean global load, loads should not drop to zero, there is no obvious thick ice inclusion or open water, and at least 7 panels need to be

active, with loads exceeding 50 kN during the crushing. The resulting ice crushing events are summarized in Table 1, and the time series for one such event in shown in Figure 2.

Table 1. List of high-speed brittle crushing events selected for further analysis.

| Date [yy-mm-dd]	Time start	Time stop	Mean load [kN]	Mean pressure [kPa]	Peak pressure [kPa]	Mean thickness [m]	Drift direction [°]
00-03-03	17:50:00	18:08:20	875	409	833	0.30	90
00-03-03	18:35:00	18:40:00	753	381	628	0.28	90
00-03-03	19:02:30	19:04:30	852	175	256	0.68	90
00-03-03	19:15:30	19:18:30	725	317	503	0.32	90
00-03-03	20:23:04	20:54:51	840	263	443	0.45	90
02-03-21	20:20:30	20:23:00	1336	265	473	0.73	45
03-03-19	21:54:20	21:55:45	1739	292	451	0.86	45
03-03-19	21:56:55	21:57:55	1144	304	525	0.54	45
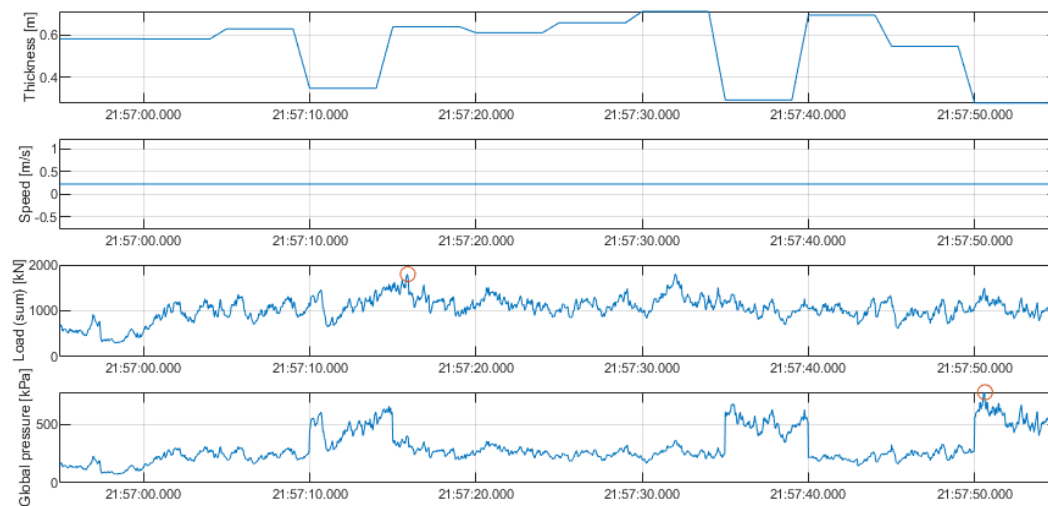
Figure 2. The ice thickness, speed, global load and global pressure for the final event in Table 1. The global pressure shown is calculated for the simultaneously occurring global load and ice thickness. The peak load and peak pressure are marked in the respective plots.

Due to the large relative uncertainty in ice thickness compared to load, the peak pressure during each brittle crushing event will often be found at the point in time that happens to have the lowest ice thickness measurement, as seen in Figure 2. Thus, a crushing event that is too short can potentially exaggerate the pressure. Because there is no immediate connection between the measured ice thickness and the load at any one point in time, due to the 6-10 m distance between the thickness measurement and the load panels and the spatial variability across the load panels, using the simultaneous thickness measurement to calculate the pressure will not be accurate. Therefore, the mean thickness was used, and the peak pressure $p_{max,BC}$ was found as:

$$p_{max,BC} = \frac{F_{max,BC}}{h_\mu w_p}, \tag{4}$$

where $F_{max,BC}$ is the peak global load during each crushing event, w_p is the projected width of the structure and h_μ is the mean thickness during each crushing event. The projected width was

6.94 m and 7.18 m for drift directions of 45° and 90° respectively, due to the placements of the load panels. The mean ice pressure $p_{\mu,BC}$ during each event was found as:

$$p_{\mu,BC} = \frac{F_{\mu,BC}}{h_\mu w_p},$$ [5]

where $F_{\mu,BC}$ is the mean global load during the crushing event.

Data uncertainty
During the data analysis we encountered at least the following additional uncertainty:
- The ice thickness measurements were done 6-10 meters from the lighthouse depending on the year. Consequently, they only yield an indication of the thickness during the time of loading, but not the thickness at the actual moment of peak load. Also, as the ice thickness measurements were found to vary at the meter scale (length) often by about 0.1 m during crushing, the thickness was never the same over the entire circumference of the lighthouse. When plotting against ice thickness, or defining for example instantaneous properties (peak pressures) the uncertainty due to this measurement can be up to 25% for an ice thickness of 0.3 m.
- Measurements of drift directions were just as rare as ice speed measurements, and sometimes not corresponding with the loaded panels. The panel loads are projected onto the drift direction and may be affected by inaccuracies in the direction. Additionally, the pressure calculation may be off by at most 20% if less contact can be accounted for, such that the projected width becomes incorrect.
- We have no data from all directions for full seasons, which means we cannot judge if the specific events found are representative of annual maxima.

3. Theory and full-scale observations of the velocity effect
Relevant aspects of the theoretical framework we adopted for synchronization are introduced in Section 3.1, and in Section 3.2 full-scale observations of the velocity effect are introduced to substantiate a range of values for the ratio between the maximum synchronized load at low speed and the mean brittle crushing load at high speed.

3.1 Theoretical framework
The theoretical framework adopted here states that ice loads on a rigid structure are largest at a low speed where the failure mode transitions from ductile to brittle (Owen et al., 2023). Compared to the peak loads at higher speeds, less time is needed to allow the ice to support the relatively high load at the ductile-brittle transition. This can be interpreted as a 'rapid strengthening' of the ice, where the term 'strengthening' is loosely applied to describe the observations of a higher load at ice failure. The term encompasses the effects of both an increase in contact area and redistribution of pressure, as the mechanism responsible for the rapid increase in load is unknown. The effect is observed when the relative velocity between ice and structure remains low for sufficiently long, such as during intermittent crushing, seen in Figure 4. In nature, this can happen more frequently for compliant structures compared to rigid structures, as a greater range of conditions can lead to low relative velocities. However, note that the same maximum load can theoretically appear on rigid and flexible structures if all possible ice speeds are considered.

A simulated example comparing a flexible and rigid structure in the same ice conditions is shown in Figure 3. Clearly the rigid structure data suggests the peak loads develop at high speed during continuous crushing, but the potential of the ice is only observed on the flexible

structure where the motion of the structure causes the relative velocity to remain small for a longer time and a load increase of 30% manifests itself right before the ice floe comes to a stop.
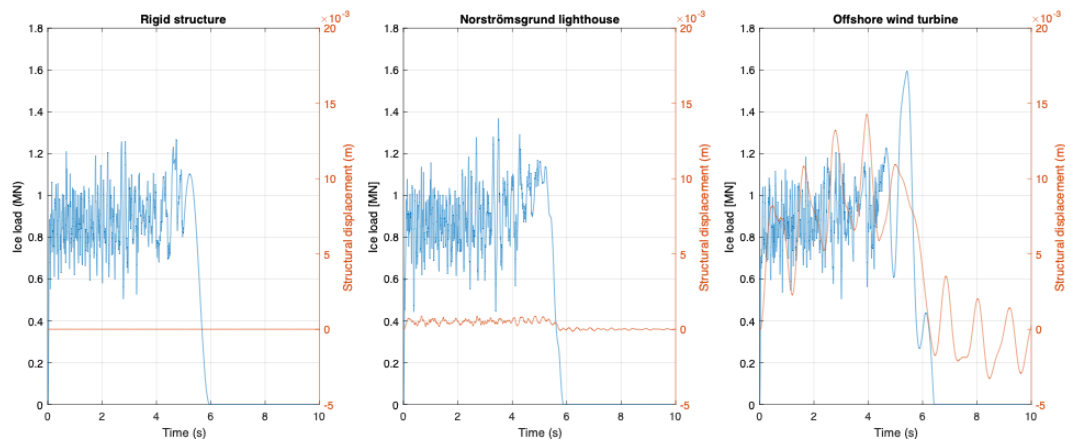

Figure 3. Example of an ice floe stopping against a completely rigid structure (left), a model of the Norströmsgrund lighthouse (middle), and a flexible wind turbine (right). Simulations made with the model developed by Hendrikse and Nord (2019).

3.2 Ratio of the low-speed maximum load to the high-speed mean brittle crushing load
Here we present full-scale data that show typical ratios of the mean high-speed brittle crushing load and the low-speed maximum load. The ratio of the peak stopping load to previous mean brittle crushing load is shown in Table 2. The best examples are found in ice floe stopping events. Data from Cook Inlet (Peyton, 1968), the Molikpaq 12 May 1986 event (Gagnon, 2012), and the Norströmsgrund lighthouse are shown in Figure 4 and 5. Observations of intermittent crushing could also be used to estimate this ratio. This data can be amended with model-scale experiments where intermittent crushing was observed such as for two examples given in Figure 6. Plenty more examples can be found in literature.
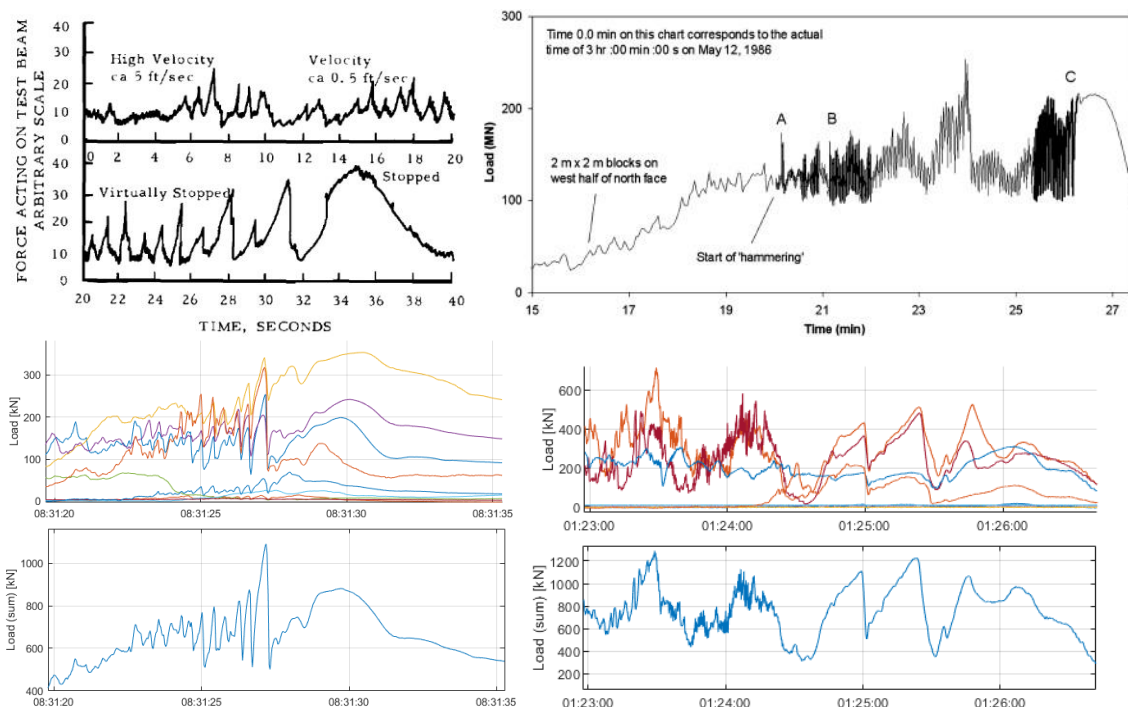

Figure 4. Top left, ice floe slowing down against a Cook Inlet test pile. Figure adapted from Peyton (1968). Top right, ice floe slowing down against the Molikpaq. Figure adapted from

Gagnon (2012). Bottom left and right, instances of ice load synchronization against the Norströmsgrund lighthouse, shown from panel loads (top) and global load (bottom). The stopping event in the bottom right has limited panel coverage, but transitions through several interaction modes before the load becomes static.

Table 2. Ratios of maximum low-speed load to mean brittle crushing load from model-scale and full-scale data.

| Source	Ratio	Note
Cook Inlet (Peyton, 1968)	~4	Figure 4.
Molikpaq (Gagnon, 2012)	~2	The piece of ice breaking off around 24 minutes may cause the mean high-speed load to be somewhat overestimated. This factor is therefore a lower estimate (Figure 4).
Norströmsgrund (this paper)	~1.7	This is a relatively low ratio, but the stopping event is quick (Figure 4) The structure is quite rigid, meaning the true potential is not revealed as illustrated in Figure 3.
Norströmsgrund (Schwarz and Jochmann, 2001)	~3	A startup event with partial panel coverage illustrating the how the loads on the lighthouse could also increase to high values after a period of very slow loading (Figure 5).
Model-scale at Aalto Ice Tank (Owen et al., 2023)	~3 – 4	The last peak load is very high due to a very small deceleration (very slow stop).
Model-scale Iowa (Hirayama et al., 1973)	~1.7	Figure 6. An example of intermittent crushing where the last peak reaches a ratio of 2.3. This is a lower bound estimate of what is possible for the given conditions.
Model-scale CRREL (Sodhi, 2001)	~4	Figure 6. There are more examples in the original work.
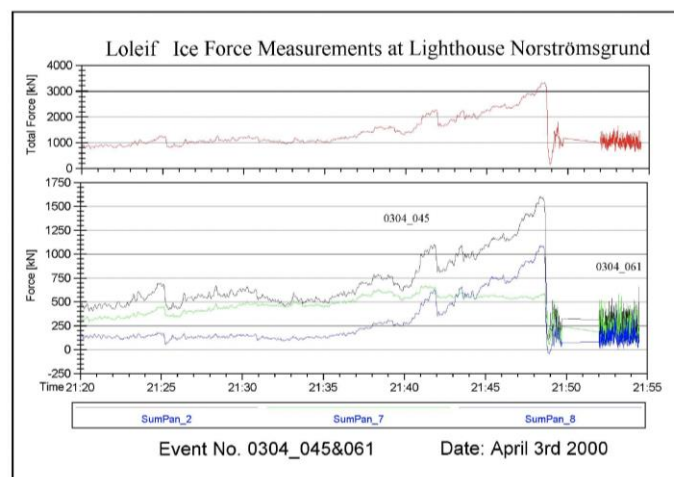
Figure 5. Example of a large factor between the low-speed load and following mean brittle crushing load after a period of an ice floe being stopped or moving very slowly against the lighthouse (Schwarz and Jochmann, 2001).
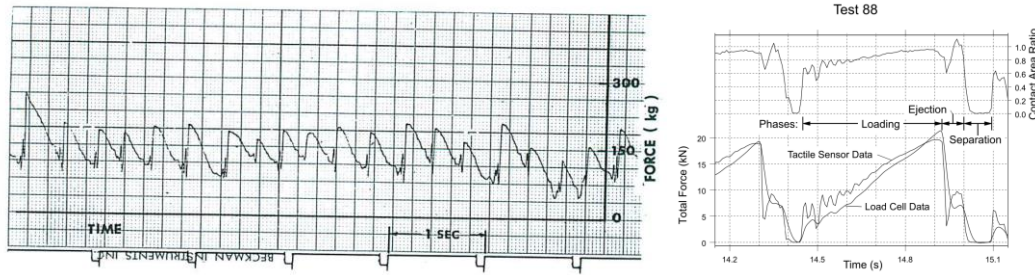
Figure 6. Examples of intermittent crushing from experimental campaigns. Left figure adapted from Hirayama et al., 1973. Right figure adapted from Sodhi et al., 2001.

4. Determination of the theoretical low speed synchronized loads based on the mean high-speed crushing loads from the lighthouse data

Based on the analysis in the previous section we estimate a factor 3 – 4 times the high-speed mean brittle crushing load to give a good indication of what the peak loads in certain conditions might be if the velocity becomes low for sufficiently long to activate the velocity effect. In Figure 7 we apply these factors to the global load events in Table 1 for which the high-speed mean brittle crushing load could be found, to estimate the theoretical low speed synchronized peak pressures.
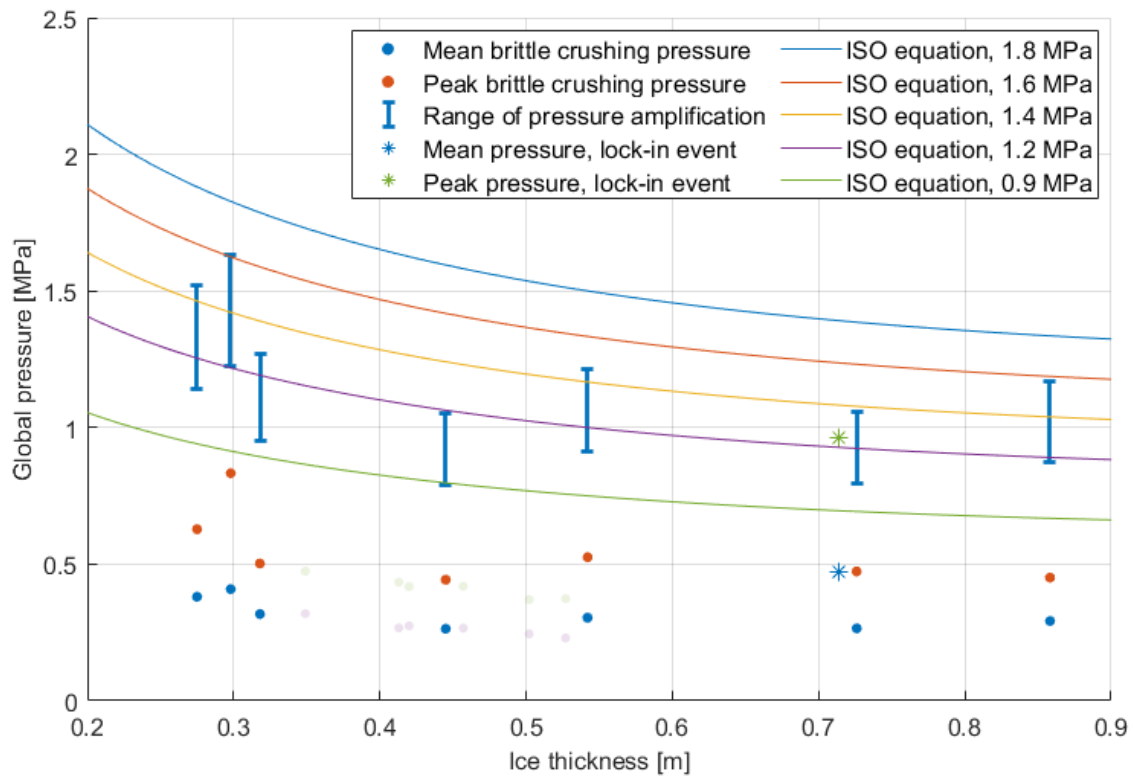

Figure 7. The mean (blue, round points) and peak (red, round points) global pressures as a function of ice thickness for high-speed brittle crushing events at Norströmsgrund given in Table 1. The solid, vertical lines above each point show the range 3-4 times mean pressures. The curves are plots of the ISO crushing equation (Eq. 2) for C_R values of 0.9 to 1.8 MPa. The translucent points between 0.35 m and 0.53 m show the mean and peak pressures of subdivisions of the long duration event at 0.45 m thickness. The starred points show the mean and peak pressure during an instance of lock-in.

Depending on the assumed degree of synchronization, low speed loads are expected to be possible in the range from (expressed in C_R) 0.9 to 1.6 MPa, provided crushing develops. For very severe static events one may expect higher values. Note that we do not have a good idea of how high or low the mean pressures are, as it could be that our selection criteria have led to only selecting 'weak' ice. However, comparing the associated peak pressures in Figure 7 with those in Figure 1 do not indicate that this is the case. An interesting lock-in event to consider which seems to fall a bit outside this realm of measurement is treated in the discussion.

5. Discussion

This study proved to be more complicated than originally expected. The events and methods associated with the global pressure values shown in Figure 1 were not found in the report by Kärnä and Qu (2006) that Kärnä and Masterson (2011) cited. Thus, the original dataset had to be reanalyzed to find brittle crushing events which had relatively certain environmental data (ice thickness, velocity) and panel loads. Only eight time series resulted from the analysis with our requirements, which may be attributed to:

- Our requirements being more stringent, especially in terms of environmental data. For example, it is possible that they extrapolated environmental data, or estimated the full ice thickness from only ice draft measurements.
- Selection of events. To reduce uncertainty, we preferred longer events of brittle crushing where possible, while selecting shorter sub-events could produce more events.

Selecting sub-events which happened to have low, simultaneously measured ice thickness could also inflate the peak pressures. A demonstration of this phenomenon can be seen in the translucent points in Figure 7, where sub-sampling a crushing event results in a relatively large range of ice thicknesses and associated pressures. The sub-sampling illustrates the significant degree of uncertainty associated with plots like Figure 1 and Figure 7, and the need to account for that uncertainty when using them as a basis for design.

An interesting lock-in event was found during the reanalysis with pressures significantly higher than brittle crushing at equivalent thickness, shown in Figure 7. The event itself (Figure 8) seems to have had significant pressure amplification due to synchronization and is a good example of a type of event that must be considered during design. The interaction seems to start after a circumferential crack, which may have prepared the surface such that good contact between the incoming ice sheet and structure occurred.
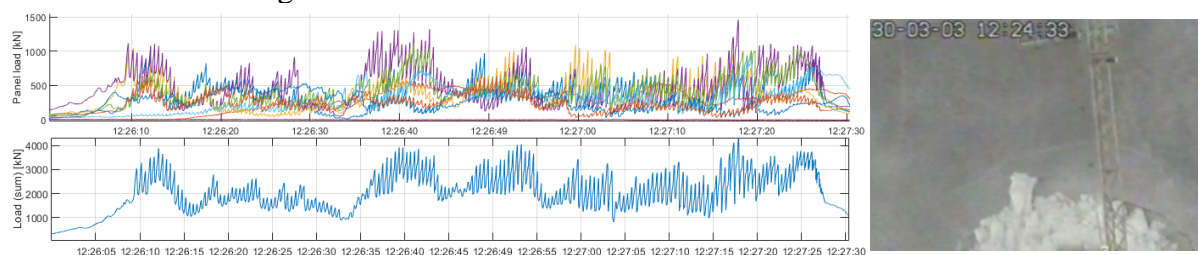

Figure 8. Left: The force-time series of a lock-in event at the lighthouse. Right: an image of the surveillance video from the lighthouse showing circumferential cracks appearing in the bottom right, before the leading edge hits the structure and lock-in occurs.

During the analysis, we found synchronized load increases, intermittent crushing (though only on part of the structure) and lock-in. All yielding relatively high loads in their respective time series. As such, the lighthouse behaved rigid, but not fully rigid under high loading and thick ice which could sustain the loading. The rigidity did however mean that the lighthouse did not

show the maximum force that could potentially develop during most interactions with ice. Thus, there is the risk that statistical methods based purely on this dataset may inherently underpredict the maximum load that may develop.

From our results, the 1-year nominal value of 1.8 MPa proposed by Kärnä and Masterson (2011) is somewhat high, it lies in the range of 5 – 6 times the mean global crushing pressure. The magnitude of this increase does mirror observations from full-scale tests with perfect full-thickness initial contact (Croasdale, 1977; Sodhi, 1998). The 1-year value of 1.34 MPa proposed by Thijssen and Fuglem (2015) falls in the range of three to four times the mean crushing pressure due to synchronization, which is the higher end of what has been observed for stopping events and intermittent crushing in full-scale and model-scale. The 1-year value of around 0.75 MPa for the Bay of Bothnia by Gravesen and Kärnä (2009) reflects an average value for two times synchronization, which underestimates the potential for synchronized loading at low speed on rigid structures. A sidenote to make here is that Gravesen and Kärnä do propose to increase this value to account for compliance of the structure, which means inherently accounting for a lower probability of low-speed conditions on a rigid structure. For a very compliant structure this value would increase to 1.5 MPa which puts it in the upper range of four times the mean global crushing pressure.

Based on our results, the value of 1.34 MPa proposed by Thijssen and Fuglem (2015) can be assumed to account for synchronized loading at low speed already and reflects what can be expected during intermittent crushing for the location of the lighthouse. Values below 0.9 MPa in any location in the Baltic may not be justified to sufficiently account for synchronization based on our analysis, though it must be stated that we could only use a limited set of measurements where the global loads could be obtained, and lower mean pressures would allow for a lower value. Also, a value lower than 0.9 MPa could theoretically be justified for a rigid structure if one could find a way to account for the actual probability of having sustained low-speed loading. The latter has not been possible so far.

6. Conclusion
Low-speed global peak loads for a structure at the location of the Norströmsgrund lighthouse in conditions encountered during the measurement campaigns between 1999 and 2003 are estimated. The estimation is based on a theoretical framework that explains the velocity effect as a rapid 'strengthening' of ice at near-zero loading velocity. The framework suggests that the ratio of the maximum load the ice can exert on a structure at low speed to the mean load during high-speed brittle crushing has a relatively narrow range. Full-scale and model-scale data suggest that this factor could be in the range of 3 – 4, depending mostly on the duration of low-speed loading and structural compliance.

Applying the factor 3 – 4 to high-speed mean brittle crushing loads measured on the Norströmsgrund lighthouse shows that, for the time series analyzed, a C_R value of 1.6 MPa used in Eq. 2 gives a good indication of the maximum global pressures that could have developed for different ice thicknesses on a very flexible structure at the same location and in the same conditions, or in case of sustained low speed loading on a rigid structure. This value is somewhat lower than the 1.8 MPa suggested for this purpose in ISO 19906. A case of frequency lock-in with high contact between ice and structure due to repetitive bending failure creating a smooth ice edge demonstrates, however, that there may always be scenarios which may yield loads significantly above this level.

Based on this analysis it is recommended to not design structures in the Baltic Sea (for the ultimate or accidental limit states) for a nominal C_R representative of the 1-year maximum less than 0.9 MPa, reflecting a typical synchronized interaction (three time the high-speed mean load) with a relatively weak ice floe as encountered at the Norströmsgrund lighthouse. That value then accounts for all possible loading effects (velocity, compliance) except the internal dynamic amplification in the structure.

References

Bjerkås, M., 2006. Ice action on offshore structures. Ph.D. thesis. NTNU, ISBN 82-471-7756-0.

Croasdale, K., 1977. Ice engineering for offshore petroleum exploration in Canada. Proc. 4th International Conference on Port and Ocean Engineering Under Arctic Conditions, St. John's, Canada.

Fransson, L., 2001. Development of Ice Load Panels and Installations at Lighthouse Norstrømsgrund. LOLEIF Report No. 5-A.

Gagnon, R.E., 2012. An explanation for the Molikpaq May 12, 1986 event. Cold Regions Science and Technology, 82, pp.75-93.

Gravesen, H. and Kärnä, T., 2009. Ice loads for offshore wind turbines in Southern Baltic Sea. Proc. 20th International Conference on Port and Ocean Engineering Under Arctic Conditions, Luleå, Sweden.

Hendrikse, H. and Owen., C.C., 2023. Application of the suggested ice strength coefficients in ISO 19906 to intermittent crushing. Proc. 27th International Conference on Port and Ocean Engineering Under Arctic Conditions, Glasgow, United Kingdom.

Hendrikse, H. and Nord, T., 2019. Dynamic response of an offshore structure interacting with an ice floe failing in crushing. Marine Structures 65, 271-290.

Hirayama, K., Schwarz., J. and Wu., H., 1973. Model technique for the investigation of ice forces on structures. Proc. 2nd International Conference on Port and Ocean Engineering Under Arctic Conditions, Reykjavik, Iceland.

Hornnes, V., Høyland, K.V., Turner, J.D., Gedikli., E.D. and Bjerkås, M., 2020. Combined distribution of ice thickness and speed based on local measurements at the Norströmsgrund lighthouse 2000-2003. Proc. 25th IAHR International Symposium on Ice, Trondheim, Norway.

ISO19906, 2019. Petroleum and natural gas industries – Arctic offshore structures. International Organization for Standardization, Geneva, Switzerland.

Kärnä, T. and Masterson, D.M., 2011. Data for crushing formula. Proc. 21st International Conference on Port and Ocean Engineering Under Arctic Conditions, Montréal, Canada.

Kärnä, T. and Qu, Y., 2006. Analysis of the size effect in ice crushing – edition 2. Version 1.3, 26-08-2009. VTT Internal report. RTE50-IR-6/2005.

Owen, C.C., Hammer, T.C. and Hendrikse, H., 2023. Peak loads during dynamic ice-structure interaction caused by rapid ice strengthening at near-zero relative velocity. Cold Regions Science and Technology, 211, p.103864.

Peyton, H.R., 1968. Sea ice forces. NRC of Canada, Technical Memorandum 92.

Schwarz, J., and Jochmann, P., 2001. Ice force measurements within the LOLEIF project. Proc. 16th International Conference on Port and Ocean Engineering Under Arctic Conditions, Ottawa, Canada.

Sodhi, D.S., Takeuchi, T., Nakazawa, N., Akagawa, S. and Saeki, H., 1998. Medium-scale indentation tests on sea ice at various speeds. Cold Regions Science and Technology, 28(3), pp.161-182.

Sodhi, D.S., 2001. Crushing failure during ice–structure interaction. Engineering Fracture Mechanics, 68(17-18), pp.1889-1921.

Thijssen, J. and Fuglem, M., 2015. Methodology to evaluate sea ice loads for seasonal operations. Proceedings of the ASME 2015 34th International Conference on Ocean, Offshore and Arctic Engineering, St. John's, Canada.